

Dynamical local-field factors and effective interactions in the three-dimensional electron liquid

C. F. Richardson and N. W. Ashcroft

Laboratory of Atomic and Solid State Physics and Materials Science Center, Cornell University, Ithaca, New York 14853-2501

(Received 22 February 1994)

We present a study of the local-field factors for the homogeneous, isotropic, three-dimensional interacting electron liquid as a function of momentum, imaginary frequency ($i\omega$), and density (r_s). A variational approach is used to solve integral equations for the density-density and spin-spin response functions, and it provides approximations to the local-field factors which are exact in the high-density limit. We derive sum rules which show that for large $i\omega$, the local-field factors possess maxima (in both q and $i\omega$) whose magnitudes are related to the pair-distribution function evaluated at zero separation. We introduce a parametrization scheme which incorporates these sum rules with the known compressibility, susceptibility, and third-moment sum rules. The local-field factors are then used to calculate the effective electron-electron interaction using the Vignale-Singwi formalism [Phys. Rev. B **32**, 2156 (1985)]. It is found to be significantly larger than that predicted by Hubbard-type local-field factors for small to intermediate values of the wave vector and imaginary frequency.

I. INTRODUCTION

In many of the problems in condensed-matter physics concerned with electronic structure, it is useful to describe the many-body effects of screening, exchange, and correlation in terms of an effective two-body electron-electron interaction. Kukkonen and Overhauser¹ have provided a physically motivated expression for this effective interaction in the homogeneous interacting electron-gas problem. Their expression is derived by considering the rearrangement of electrons in the vicinity of a test charge; the rearranged electrons constitute a charge cloud with which other particles interact through a direct Coulomb term, but also through an exchange and correlation term. This exchange and correlation term is assumed to be proportional to the direct interaction term where the constant of proportionality is termed a local-field factor. These local-field factors can be rigorously defined in terms of the response functions and their determination provides a useful starting point for understanding the role of many-body effects in the interacting electron-gas.

Although many approximations for the static local-field factors in the interacting electron-gas problem are available in the literature, relatively few address the issue of the frequency dependence of the local-field factors. The importance of this frequency dependence is demonstrated by the fact that it is not possible to simultaneously satisfy the compressibility sum rule and the third-moment sum rule using static local-field factors. It is also reflected in the lifetime of the volume plasmon; when static local field factors are used, the plasmon lifetime is predicted to be infinite for a momentum less than the smallest momentum permitting both energy and momentum to be conserved in a single electron-hole pair decay. In reality, however, the plasmon has a finite lifetime, even for smaller values of momenta, and this implies that the local-field factors possess imaginary parts; in turn this implies that they are frequency dependent. This paper will

therefore be directed towards an approximate determination of the local-field factors of the interacting electron gas. In a later publication,² the results of this paper will be applied to the problem of superconducting order in the electron gas.

In determining the local-field factors, we will begin by using a microscopic theory based on a summation of an infinite class of diagrams within many-body perturbation theory. This method has the usual disadvantage that at sufficiently low densities it will necessarily be inaccurate. We overcome this difficulty by parametrizing the local-field factors in such a way that they approximately approach the results of the microscopic theory for high densities, but also *exactly* satisfy the compressibility, susceptibility, and the third-moment sum rules at all densities. We find it convenient to work with imaginary frequencies not only because the numerical work is thereby simplified but also because this framework is needed in many calculations in the electron gas. We also derive new sum rules for the local-field factors for large imaginary frequency. These state that when $\hbar^2 q^2/2m = \hbar\omega$, the corresponding local-field factors approach a local maximum value which can be expressed in terms of the radial distribution evaluated at zero separation.

In Sec. II, we determine the local-field factors using linearized vertex equations^{3,4} to sum self-energy, exchange, and fluctuation terms in the diagrammatic expansion of the vertex functions. These integral equations are solved by a variational method^{4,5} within a local approximation. The variational solutions of the vertex equations are simply related to the leading order (in the screened interaction) polarization diagrams. The results for the response functions exactly reproduce the first-order correction to the random-phase approximation (RPA) result, but in addition also approximately include an infinite class of higher-order corrections. Knowledge of the vertex functions then allows the local-field factors to be calculated. Our results for the spin-antisymmetric local-field factor G_a reproduce those of Brosens and co-

workers⁶ and Devreese, Brosens, and Lemmens,⁷ except that the internal Coulomb lines are screened in our calculation. The spin-symmetric local-field factor G_s also includes fluctuation diagrams. The first step in evaluating these polarization diagrams is to separate out the first-order diagrams, which can be reduced to one-dimensional integrals. The remaining diagrams are related to three-dimensional integrals over the three-point function $\Lambda_0^{(3)}(\vec{p}, \vec{q})$ (see below) and for this purpose we have calculated this three-point function analytically.

Since our procedure includes correlations, several features appear here that do not arise in the Hartree-Fock approach. Most notable is the fact that the local-field factors will diverge at large momenta *unless* the Lindhard function is modified to include the effects of interactions on the occupation numbers n_q , an observation that is consistent with the findings of Vignale.⁸ We therefore modify the Lindhard function through the choice of a new local-field factor G_n and then derive exact sum rules for G_n and also give a simple parametrization of it. A further result is that the limit of small momentum of the spin-antisymmetric local field factor is, for a finite frequency, a finite negative number. This has been previously predicted on the basis of the third-moment sum rule.⁹ We find that the small- q sum rules are well satisfied for relatively high densities, e.g., for $r_s < 4$. Our calculation indicates that Hubbard-like approximations significantly underestimate the static local-field factors for intermediate values of wave vector. In Sec. III, we give a simple parametrization of the local-field factors which satisfy the sum rules exactly, have a realistic form for intermediate wave vector, and are dependent on imaginary frequency.

Many calculations incorporating local-field factors involve an effective electron-electron interaction. Procedures for calculating this effective electron-electron interaction in an electron gas have been proposed by Kukkonen and Overhauser¹ (KO) and also by Vignale and Singwi¹⁰ (VS). These procedures result in effective interactions which can be expressed in terms of the spin-

symmetric and the spin-antisymmetric local-field factors. The KO and VS equations indicate three main sources of contributions to these effective interactions: the direct Coulomb interaction, interactions arising from exchange of charge fluctuations, and interactions arising from exchange of spin fluctuations. Some earlier expressions for the effective interactions¹¹ depended only on the spin-symmetric local-field factor and suffered from the defect of including direct and exchange contributions in an inconsistent way. For densities lower than a critical density where the compressibility vanishes, these effective interactions then contain physically implausible singularities. Since the KO and VS expressions include direct and exchange contributions in a consistent manner, they entail no physically implausible singularities.

In Sec. IV effective interactions which include dynamical local-field factors are discussed and compared with those obtained using Hubbard-like static local-field factors.

II. CALCULATION OF LOCAL-FIELD FACTORS

In what follows we calculate the local-field factors from approximate integral equations^{3,4} determining the spin-spin and the density-density response functions. These integral equations are represented diagrammatically in Fig. 1. They include RPA screened-exchange and self-energy lines. However, the integral equation for the density-density response function also includes fluctuation diagrams. By using an integral equation to approximately sum an infinite number of diagrams, we can considerably extend the density range where perturbation theory is accurate. However, as noted, at sufficiently low density the neglected diagrams will eventually become important.

The solution to the integral equations is obtained by a variational approach.^{4,5} We start by noting that the integral equations^{3,4} are given by [see Figs. 1(a) and 1(b)]

$$\Lambda^{s,a}(\vec{p}, \vec{q}) = 1 - \text{Tr}_{\vec{p}} [v_{\text{RPA}}(\vec{p} - \vec{p}') + \Gamma^{s,a}(\vec{p}, \vec{p}'; \vec{q})] G_0(\vec{p}' + \vec{q}) G_0(\vec{p}') \Lambda^{s,a}(\vec{p}', \vec{q}) - \Lambda^{s,a}(\vec{p}, \vec{q}) \text{Tr}_{\vec{p}} [G_0(\vec{p} + \vec{q}) G_0(\vec{p}' + \vec{q}) + G_0(\vec{p}) G_0(\vec{p}')] v_{\text{RPA}}(\vec{p}' - \vec{p}) , \quad (1)$$

where $\text{Tr}_{\vec{p}}$ stands for $(4E_f) \int (dw_p / 2\pi) (2k_f)^3 \int d^3p / (2\pi)^3$, v_{RPA} is the Coulomb interaction screened in the RPA approximation,

$$\Gamma^s(\vec{p}, \vec{p}'; \vec{q}) = \text{Tr}_{\vec{k}} v_{\text{RPA}}(\vec{k}) v_{\text{RPA}}(\vec{k} + \vec{q}) G_0(\vec{k} - \vec{p}) [G_0(\vec{p}' - \vec{k}) + G_0(\vec{k} + \vec{p}' + \vec{q})] , \quad (2)$$

and

$$\Gamma^a = 0 . \quad (3)$$

Except where otherwise noted, we will express all momenta in units of $2\hbar k_f$ and all energies in units of $4E_f = 2\hbar^2 k_f^2 / m$. In addition, we will use the four-vector notation, namely, $\vec{q} = (iw_q, \mathbf{q})$ and $q = |\mathbf{q}|$. Equation (1) can be written as

$$\text{Tr}_{\vec{p}} K_q^{-s,a}(\vec{p}, \vec{p}') \Lambda^{s,a}(\vec{p}', \vec{q}) = 1 , \quad (4)$$

where

$$K_q^{s,a}(\vec{p}, \vec{p}') = \delta(\vec{p} - \vec{p}') \{ 1 + \text{Tr}_{\vec{p}''} v_{\text{RPA}}(\vec{p}'' - \vec{p}) [G_0(\vec{p}) G_0(\vec{p}'') + G_0(\vec{p} + \vec{q}) G_0(\vec{p}'' + \vec{q})] \} + G_0(\vec{p}' + \vec{q}) G_0(\vec{p}') [v_{\text{RPA}}(\vec{p}' - \vec{p}) + \Gamma^{s,a}(\vec{p}', \vec{p}; \vec{q})] . \quad (5)$$

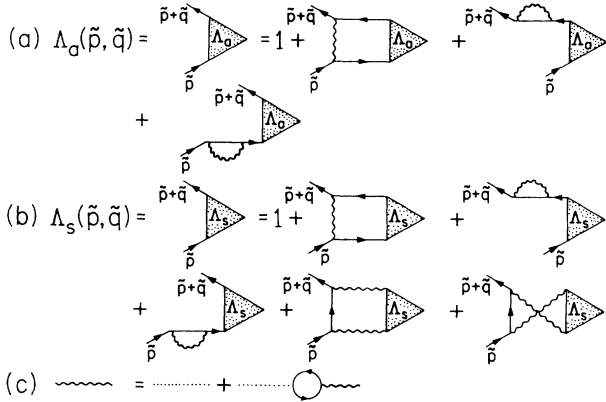


FIG. 1. Diagrammatic representations of (a) the integral equation for the spin-antisymmetric vertex function and (b) the integral equation for the spin-symmetric vertex functions. (c) shows the diagrammatic representation of the screened interaction lines.

Here, as in Eq. (1), $G_0(\vec{q}) = (4E_f)^{-1}(i\omega_q - q^2 + \mu)^{-1}$ is the Green's function of the noninteracting system. Next, we note that Eq. (4) also results from the vanishing of a functional derivative, i.e.,

$$\frac{\delta F^{s,a}[\Lambda]}{\delta \Lambda} = 0, \quad (6)$$

where

$$\begin{aligned} F^{s,a}[\Lambda] = & \text{Tr}_{\vec{p}} \text{Tr}_{\vec{p}'} \Lambda^{s,a}(\vec{p}, \vec{q}) G_0(\vec{p} + \vec{q}) \\ & \times G_0(\vec{p}) K_q(\vec{p}, \vec{p}') \Lambda^{s,a}(\vec{p}', \vec{q}) \\ & - 2 \text{Tr}_{\vec{p}} G_0(\vec{p} + \vec{q}) G_0(\vec{p}) \Lambda^{s,a}(\vec{p}, \vec{q}). \end{aligned} \quad (7)$$

By taking a trial solution $\Lambda^{s,a}(\vec{p}, \vec{q}) = \Lambda^{s,a}(\vec{q})$ (this is the local approximation) we find

$$\Lambda^s(\vec{q}) = \frac{\Pi_0(\vec{q})}{\Pi_0(\vec{q}) - \Pi_{\text{se}}(\vec{q}) - \Pi_{\text{ex}}(\vec{q}) - \Pi_{\text{fl}}(\vec{q})} \quad (8)$$

and

$$\Lambda^a(\vec{q}) = \frac{\Pi_0(\vec{q})}{\Pi_0(\vec{q}) - \Pi_{\text{se}}(\vec{q}) - \Pi_{\text{ex}}(\vec{q})}. \quad (9)$$

The expression for the spin-spin vertex function is therefore the same as that of Refs. 6 and 7, except that here the internal lines in our function are screened. The expression for the density-density vertex function contains

$$\begin{aligned} \Pi_{\pm}(q, i\omega) = & \frac{1}{(4\pi a_0)^3 (e^2/2a_0)} \\ & \times \text{Re} \left\{ \int_{-1}^1 dz \int_{-1}^1 dz' \frac{1}{(i\omega + q^2 + qz)(\pm i\omega + q^2 + qz')} \right. \\ & \left. \times \left[\frac{1}{2} \mathcal{W}_{\pm}(z, z') - \frac{1}{2} (u + v + s_{\pm}^2) + 2v \ln \left| \frac{u - v + s_{\pm}^2 + \mathcal{W}_{\pm}(z, z')}{2s_{\pm}^2} \right| \right] \right\}. \end{aligned} \quad (13)$$

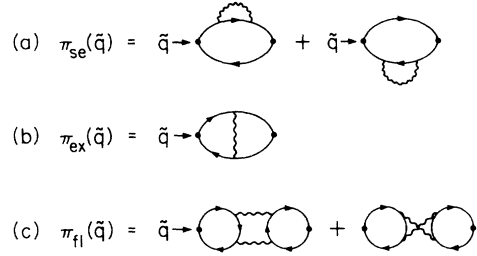


FIG. 2. The polarization diagrams required in the calculation of the local-field factors; (a) shows the self-energy diagrams, (b) shows the exchange diagram, and finally, (c) shows the fluctuation diagrams.

the additional term $\Pi_{\text{fl}}(\vec{q})$. The terms $\Pi_{\text{se}}(\vec{q})$, $\Pi_{\text{ex}}(\vec{q})$, and $\Pi_{\text{fl}}(\vec{q})$ are shown in Fig. 2 and can be otherwise expressed as

$$\begin{aligned} \Pi_{\text{se}}(\vec{q}) = & -2 \text{Re} \text{Tr}_{\vec{p}} \text{Tr}_{\vec{k}} v_{\text{RPA}}(\vec{p}) G_0(\vec{k}) \\ & \times G_0^2(\vec{k} + \vec{q}) G_0(\vec{k} + \vec{q} + \vec{p}), \end{aligned} \quad (10)$$

$$\begin{aligned} \Pi_{\text{ex}}(\vec{q}) = & -2 \text{Tr}_{\vec{p}} \text{Tr}_{\vec{k}} v_{\text{RPA}}(\vec{p}) G_0(\vec{k}) G_0(\vec{k} + \vec{q}) \\ & \times G_0(\vec{k} + \vec{q} + \vec{p}) G_0(\vec{k} + \vec{p}), \end{aligned} \quad (11)$$

where $\Pi_{\text{fl}}(\vec{q})$ is given later in Eq. (25).

The problem of calculating the local-field factors has now been reduced to evaluating the three types of low-order polarization diagrams shown in Fig. 2. In order to compute these diagrams, we separate them into first-order diagrams and higher-order diagrams. The first-order diagrams can be simplified by following the method of Ref. 6 and writing the momentum integrals in cylindrical coordinate. By proceeding this way, Broens and co-workers⁶ were able to obtain a two-dimensional integral for the diagrams. For the special case of $w=0$, the first-order diagrams have been expressed in terms of one-dimensional integrals by Engel and Vosko.¹² We are able to extend these results by reducing all first-order diagrams for arbitrary frequency and momenta to one-dimensional integrals. By extending the result of Ref. 6 to imaginary frequencies, the first-order correction to the response can then be written as

$$\Pi_1(q, i\omega) = \Pi_{\text{se}}^{(1)}(q, i\omega) + \Pi_+(q, i\omega) + \Pi_-(q, i\omega), \quad (12)$$

where $\Pi_{\text{se}}^{(1)}(q, i\omega)$ is the sum of first-order self-energy diagrams and

Here $u = 1 - z^2$, $v = 1 - z'^2$, $s_+ = 2q + z + z'$, $s_- = z - z'$, and

$$W_{\pm}(z, z') = [(u - v)^2 + 2s_{\pm}^2(u + v) + s_{\pm}^4]^{1/2}. \quad (14)$$

By writing

$$\frac{1}{iw + q^2 + qz} = \frac{1}{q} \frac{\partial}{\partial z} \ln(iw + q^2 + qz), \quad (15)$$

we can integrate by parts to perform one further integral and we can also reduce the self-energy expression to a one-dimensional integral by noting that after a simple frequency integration, the self-energy diagram expressed in cylindrical coordinates becomes

$$\begin{aligned} \Pi_{\text{se}}^{(1)}(q, iw) = & \frac{(k_f a_0)}{\pi^2 a_0^3 (e^2 / 2a_0)} \text{Re} \int_{-1/2}^{1/2} dz \int_0^{(1/4 - z^2)^{1/2}} d\rho \frac{\rho}{(iw + q^2 + 2qz)^2} \\ & \times \{ \Sigma_{\text{HF}}([\rho^2 + z^2 + q^2 + 2qz]^{1/2}) - \Sigma_{\text{HF}}([\rho^2 + z^2]^{1/2}) \}, \quad (16) \end{aligned}$$

where $\Sigma_{\text{HF}}(\rho)$ is the Hartree-Fock self-energy. The integral over ρ can then be performed in the first term by invoking the substitution¹² $x = [\rho^2 + z^2 + q^2 + 2qz]^{1/2}$ and in the second with the substitution¹² $x = [\rho^2 + z^2]^{1/2}$. The final result, though quite cumbersome, is nevertheless straightforward to evaluate and can be expressed as

$$\begin{aligned} \Pi_1(q, iw) = & - \frac{2}{(4\pi a_0)^3 (e^2 / 2a_0) q} \\ & \times \text{Re} \left[\left[\frac{1}{q^2} (iw + q^2 - q) \ln(iw + q^2 - q) - \frac{1}{q^2} (iw + q^2 + q) \ln(iw + q^2 + q) + \frac{2}{q} \right] \right. \\ & \times \left[-\ln(iw + q^2 + q) - \ln(iw + q^2 - q) - \frac{iw + q^2}{q} \ln \left[\frac{w^2 + q^2(q+1)^2}{w^2 + q^2(q-1)^2} \right] \right] \\ & + \frac{1}{q} [\ln^2(iw + q^2 + q) - \ln^2(iw + q^2 - q)] \\ & \times \left\{ \left[1 - \left[\frac{q^2 + iw}{q} \right]^2 \right] \ln \left[\frac{iw + q^2 + q}{iw + q^2 - q} \right] + \text{c.c.} \right\} - \frac{8}{q} \\ & - \frac{2}{q^2} \{ (iw + q^2 + q) [\ln(iw + q^2 + q) - 2] \\ & \quad - (iw + q^2 - q) \ln(iw + q^2 - q) [\ln(iw + q^2 - q) - 2] \} \\ & + 2 \int_{-1}^1 dz \frac{1 + 2 \ln(iw + q^2 + qz)}{iw + q^2 + qz} \left[(1 - z^2) \ln \left| \frac{1+z}{1-z} \right| - [1 - (2q + z)^2] \ln \left| \frac{1 + 2q + z}{1 - (2q + z)} \right| \right] \\ & - 2 \int_{-1}^1 dz \frac{1}{(1 + 4q^2 + 4qz)^{1/2} (iw + q^2 + qz)} \ln \left| \frac{1 + (1 + 4q^2 + 4qz)^{1/2}}{1 - (1 + 4q^2 + 4qz)^{1/2}} \right| \\ & \quad \times [\lambda(q, w, z) \ln(iw + q^2 + qz) + 8q^2(q + z)] \\ & \left. + 4 \int_{-1}^1 dz \frac{2q + z}{1 + 4q^2 + 4qz} \ln(iw + q^2 + qz) - 2 \int_{-1}^1 dz \frac{\ln(iw + q^2 + qz)}{iw + q^2 + qz} I(q, w, z) \right], \quad (17) \end{aligned}$$

where

$$\begin{aligned} \lambda(q, w, z) = & \frac{1}{q(1 + 4q^2 + 4qz)} [q(q + z)(1 + 20q^2 + 56q^4 + (14 + 92q^2)qz + 36q^2z^2) + 2w^2(1 + 4q^2 + 4qz) \\ & + iw(1 + 18q^2 + 48q^4 + (3 + 19q^2)4qz + 28q^2z^2)], \quad (18) \end{aligned}$$

$$\begin{aligned} I(q, w, z) = & \frac{A}{B} \left[\ln \left[\frac{2w(1 + 2q^2 + 2q + 2qz + z - |qz|)(q - 1) - iq(q^2 - 1)(2|q + z| - B)}{2w(1 + 2q^2 - 2q + 2qz - z - |q + z|)(q + 1) - iq(q^2 - 1)(2|q + z| - B)} \right] \right. \\ & \left. - \ln \left[\frac{2w(1 + 2q^2 + 2q + 2qz + z - |q + z|)(q - 1) - iq(q^2 - 1)(2|q + z| + B)}{2w(1 + 2q^2 - 2q + 2qz - z - |q + z|)(q + 1) - iq(q^2 - 1)(2|q + z| + B)} \right] \right], \quad (19) \end{aligned}$$

$$A = \frac{1}{q^2} [q^4 - 12w^2q^2 - w^2 + (q^2 - 3w^2)2qz + q^2z^2] + \frac{2iw}{q^2} [3q^2 - q^4 + w^2 + (1 + 3q^2)qz + 2q^2z^2], \quad (20)$$

and

$$B = 2 \left[(q+z)^2 - \frac{w^2}{q^2} (1 + 4q^2 + 4qz) + iw \frac{2}{q} (q+z)(1 + 2qz) \right]^{1/2}. \quad (21)$$

It should be noted that when this result is analytically continued to real w , logarithmic singularities occur when $w = q^2 \pm q$. They are, however, simply unphysical artifacts of finite-order perturbation theory, resulting from the second-order pole in the diagrams with self-energy corrections. We can see this by noting that if we had used the *full* Hartree-Fock Green's function we would have obtained

$$\Pi_0(q, w) + \Pi_{\text{se}}(q, w) = \frac{4(k_f a_0)}{a_0^3 (e^2/2a_0)} \int \frac{d^3k}{(2\pi)^3} \left[\frac{n_{\mathbf{k}}^0 - n_{\mathbf{k}+\mathbf{q}}^0}{w + i\delta + \epsilon_{\mathbf{k}} - \epsilon_{\mathbf{k}+\mathbf{q}} + \Sigma_{\text{HF}}(k) - \Sigma_{\text{HF}}(\mathbf{k}+\mathbf{q})} \right]. \quad (22)$$

At $w = q^2 \pm q$ we can evaluate leading order behavior of this expression; to do so we consider the small- r_s limit of $(k_f)^{-1} [\Pi_0(q, w = q^2 \pm q) + \Pi_{\text{se}}(q, w = q^2 \pm q)]$. Since the self-energy (here in units of $4E_f$) vanishes at $r_s = 0$, the integrand in Eq. (22) diverges for $r_s = 0$ when $k = \frac{1}{2}$ and $\cos(\theta) = \pm 1$, where θ is the angle between $\hat{\mathbf{k}}$ and $\hat{\mathbf{q}}$. To analyze the effects of this singularity for $0 < r_s \ll 1$, it is sufficient to set $k = \frac{1}{2}$ and $\cos(\theta) = \pm 1$ in the self-energies. The result is that $\Pi_{\text{se}}(q, w = q^2 \pm q)$ [and hence $G(q, w = q^2 \pm q)$] contains a term proportional to $\ln(r_s)$. Because of this nonanalytic dependence on r_s , it is clear that the result could *not* have been obtained by using finite-order perturbation theory. This is the origin of the divergence noted above and also obtained in Refs. 6 and 7. In our theory, we approximately sum the diagrams required to give Eq. (22), but our approximation is insufficiently accurate to obtain the correct behavior at $w = q^2 \pm q$. However, provided we consider extensions to imaginary frequencies no such problems arise.

All of the remaining diagrams can be described in terms of the three-point function¹³ according to

$$\begin{aligned} \Pi_{\text{sc}}(\bar{p}) &= \Pi_{\text{sc}}^{(1)}(\bar{p}) + \text{Tr}_{\bar{q}} [v_{\text{RPA}}(\bar{q}) - v_q] \\ &\quad \times \frac{1}{4E_f} \left[\frac{\partial}{\partial(iw_q)} - \frac{\partial}{\partial(iw_p)} \right] \\ &\quad \times [\Lambda_0^{(3)}(\bar{p}, \bar{q}) - \Lambda_0^{(3)}(\bar{q}, \bar{p})], \end{aligned} \quad (23)$$

$$\begin{aligned} \Pi_{\text{ex}}(\bar{p}) &= \Pi_{\text{ex}}^{(1)}(\bar{p}) + \frac{1}{2} \text{Tr}_{\bar{q}} \frac{[v_{\text{RPA}}(\bar{q}) - v_q]}{(2k_f)^2 p \cdot \mathbf{q}} \\ &\quad \times [\Lambda_0^{(3)}(\bar{p}, \bar{q}) + \Lambda_0^{(3)}(\bar{q}, \bar{p}) \\ &\quad - \Lambda_0^{(3)}(-\bar{p}, \bar{q}) - \Lambda_0^{(3)}(\bar{q}, -\bar{p})], \end{aligned} \quad (24)$$

and

$$\begin{aligned} \Pi_{\text{n}}(\bar{p}) &= -\frac{1}{2} \text{Tr}_{\bar{q}} v_{\text{RPA}}(\bar{q}) v_{\text{RPA}}(\bar{p} - \bar{q}) \\ &\quad \times [\Lambda_0^{(3)}(\bar{q}, \bar{p} - \bar{q}) + \Lambda_0^{(3)}(\bar{p} - \bar{q}, \bar{q})]^2. \end{aligned} \quad (25)$$

The three-point function $\Lambda_0^{(3)}(\bar{q}, \bar{p})$, is given by

$$\Lambda_0^{(3)}(\bar{q}, \bar{p}) = -2 \text{Tr}_{\bar{k}} G_0(\bar{k}) G_0(\bar{k} + \bar{q}) G_0(\bar{k} + \bar{q} + \bar{p}), \quad (26)$$

and once it is known, the integrals above can be evaluated numerically. An analytic form of the three-dimensional three-point function as a function of real frequency has been provided by Cenni and Saracco.¹³ The extension to imaginary frequencies, which we require, is given in the Appendix, where we also present an analytic derivation of the three-dimensional three-point function.

There are two ways to express the response functions in terms of local-field factors. The first is to write the response functions as

$$\Pi^{s,a}(\bar{q}) = \frac{\Pi_0(\bar{q})}{1 + v_q \bar{G}_{s,a}(\bar{q}) \Pi_0(\bar{q})} \quad (27)$$

and the alternative is to write

$$\Pi^{s,a}(\bar{q}) = \frac{\bar{\Pi}_0(\bar{q})}{1 + v_q G_{s,a}(\bar{q}) \bar{\Pi}_0(\bar{q})}, \quad (28)$$

where $\bar{\Pi}_0(\bar{q})$ is the Lindhard function with the particle number for the noninteracting case replaced by the interacting equivalent, i.e.,

$$\bar{\Pi}_0(\bar{q}) = \frac{4(k_f a_0)}{a_0^3 (e^2/2a_0)} \int \frac{d^3k}{(2\pi)^3} \frac{n_{\mathbf{k}} - n_{\mathbf{k}+\mathbf{q}}}{iw_q - \epsilon_{\mathbf{k}+\mathbf{q}} + \epsilon_{\mathbf{k}}}, \quad (29)$$

where $n_{\mathbf{k}}$ is the *exact* occupation number in the interacting system. Since the *exact* occupation numbers are unknown, Eq. (29) cannot be directly used to obtain $\bar{\Pi}_0(\bar{q})$; therefore a parametrization of this function is needed. Motivated by Eqs. (27) and (28), we are led to parametrize $\bar{\Pi}_0(\bar{q})$ as

$$\bar{\Pi}_0(\bar{q}) = \frac{\Pi_0(\bar{q})}{1 + v_q G_n(\bar{q}) \Pi_0(\bar{q})}. \quad (30)$$

With this choice of parametrization, we have

$$\bar{G}_{s,a}(\bar{q}) = G_{s,a}(\bar{q}) + G_n(\bar{q}). \quad (31)$$

In Sec. III, Eq. (29) will be used to derive exact limits for the new local-field factor $G_n(\bar{q})$, but for the present Eqs. (27) and (28) can simply be regarded as the definitions of the local-field factors $G_{s,a}(\bar{q})$ and $\bar{G}_{s,a}(\bar{q})$. In the second representation of the response functions the large- \mathbf{q} limits of $G_{s,a}(\bar{q})$ approach known constants,¹⁴ namely,

$$\lim_{q \rightarrow \infty} G_a(\mathbf{q}) = \frac{4g(0) - 1}{3} \quad (32)$$

and

$$\lim_{q \rightarrow \infty} G_s(\mathbf{q}) = \frac{2}{3}[1 - g(0)], \quad (33)$$

where $g(0)$ is the radial distribution function evaluated at zero separation. In contrast, the large- q limits of $\bar{G}_{s,a}(\bar{q})$ diverge as $a(r_s)q^2$. An expression for $a(r_s)$ in terms of the correlation energy is given in Eq. (52). When considering the effective electron-electron interaction it is actually more convenient to use the functions $G_{s,a}(\bar{q})$, and $\bar{\Pi}_0(\bar{q})$. This reflects the fact that if the local-field factors diverge for large q , then the effective interaction will no longer approach its correct large- q limit.

In order to actually calculate $G_{s,a}(\bar{q})$, we must determine $\bar{\Pi}_0(\bar{q})$. This is achieved by isolating the part of $\Pi_{se}(\bar{q})$ which results solely from the change of the electron occupation numbers from the noninteracting to the interacting values.⁸ To do this, we note that $\Pi_0(\bar{q}) + \Pi_{se}(\bar{q})$ can be written as

$$\begin{aligned} \Pi_0(\bar{q}) + \Pi_{se}(\bar{q}) = & E_f^{-1} \text{Re Tr} \frac{G_0(\bar{k})}{i\omega_q - q^2 - 2\mathbf{k} \cdot \mathbf{q}} \\ & + E_f^{-1} \text{Re Tr}_k \frac{G(\bar{k}) - G_0(\bar{k})}{i\omega_q - q^2 - 2\mathbf{k} \cdot \mathbf{q}} \\ & + E_f^{-1} \text{Re Tr} \frac{G_0(\bar{k})}{(i\omega_q - q^2 - 2\mathbf{k} \cdot \mathbf{q})^2} \\ & \times [\Sigma_{\text{RPA}}(\bar{k} + \bar{q}) - \Sigma_{\text{RPA}}(\bar{k})], \quad (34) \end{aligned}$$

where $\Sigma_{\text{RPA}}(\bar{k})$ is the self-energy in the RPA approximation. The first term is the Lindhard term. The second represents the change in the Lindhard function resulting from occupation number changes induced by interactions. The sum of the first two terms is therefore $\bar{\Pi}_0^{(1)}(\mathbf{q})$ and the remaining term is $\bar{\Pi}_{se}(\bar{q})$. Here $\bar{\Pi}_0^{(1)}(\bar{q})$ is the first-order (in the number of RPA lines) approximation to $\bar{\Pi}_0(\bar{q})$. We evaluate this by noting that the expression for $\bar{\Pi}_{se}(\bar{q})$ is given by an expression similar to Eq. (23), but with the three-point function modified to include the extra $\mathbf{k} \cdot \mathbf{q}$ that is present in the denominator of Eq. (34).

From Eqs. (8), (9), (28), and (30) we have

$$G_s(q, i\omega) = \frac{-1}{v_q \Pi_0^2(q, i\omega)} [\bar{\Pi}_{se}(q, i\omega) + \Pi_{ex}(q, i\omega) + \Pi_{fl}(q, i\omega)], \quad (35)$$

$$G_a(q, i\omega) = \frac{-1}{v_q \Pi_0^2(q, i\omega)} [\bar{\Pi}_{se}(q, i\omega) + \Pi_{ex}(q, i\omega)], \quad (36)$$

and

$$G_n(q, i\omega) = \frac{-1}{v_q \Pi_0^2(q, i\omega)} [\bar{\Pi}_0^{(1)}(q, i\omega) - \Pi_0(q, i\omega)]. \quad (37)$$

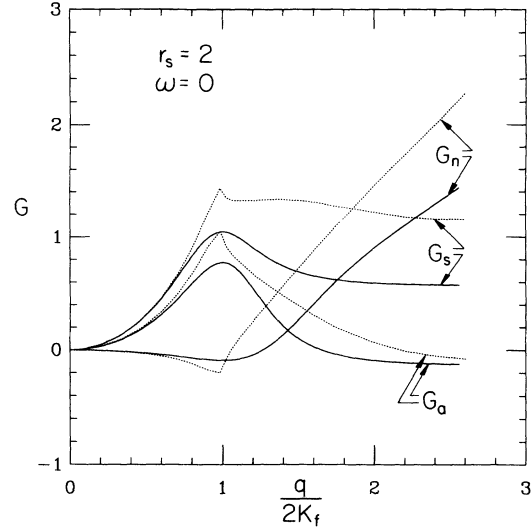


FIG. 3. Local-field factors for $r_s=2$ and $\omega=0$. The solid lines correspond to the parametrized local-field factors, Eqs. (53)–(65), and the dotted lines to the local-field factors calculated using Eqs. (35)–(37). The differences at large q are due to the failure of Eqs. (35)–(37) to adequately satisfy the large- q sum rules, in contrast to the parametrized forms, which are constrained by these rules.

The results are plotted in Figs. 3–5 at relatively high density ($r_s=2$). Since the local-field factors are only moderately sensitive to the density, the results in these figures are representative of the entire metallic density range. The local-field factors for very low densities will be discussed at more length elsewhere.²

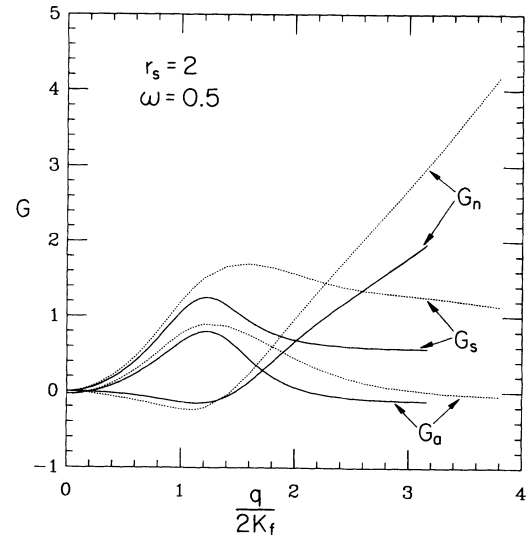


FIG. 4. Local-field factors for $r_s=2$ and $\omega=0.5$. The solid lines correspond to the parametrized local-field Eqs. (53)–(65), and the dotted lines to the local-field factors calculated using Eqs. (35)–(37). The differences at large q are due to the failure of Eqs. (35)–(37) to adequately satisfy the large- q sum rules, in contrast to the parametrized forms, which are constrained by these rules.

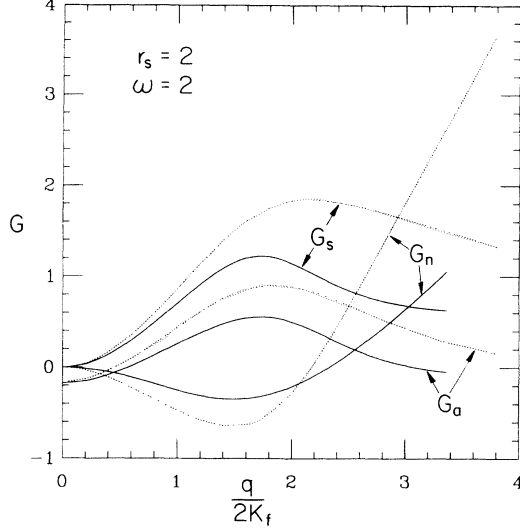


FIG. 5. Local-field factors for $r_s=2$ and $w=2.0$. The solid lines correspond to the parametrized local-field factors, Eqs. (53)–(65), and the dotted lines are the local-field factors calculated using Eqs. (35)–(37). Again, the differences at large q are due to the failure of Eqs. (35)–(37) to adequately satisfy the large- q sum rules, in contrast to the parametrized forms, which are constrained by these rules.

III. PARAMETRIZATION OF THE LOCAL-FIELD FACTORS

For practical applications, two difficulties arise with the above procedure: (i) for problems involving multidimensional integrals whose integrands depend on $G(q, iw)$, the numerical work becomes burdensome; (ii) for low densities the calculation we have described becomes inaccurate. We attempt to solve both problems by proposing a simple parametrization for the local-field factors which incorporates the known sum rules.

First, we utilize what is known *exactly* about the local-field factors. For $w=0$, we know that $G_s(q, 0) = \lambda_s^{(0)}(r_s)q^2$, $G_a(q, 0) = \lambda_a^{(0)}(r_s)q^2$, and $G_n(q, 0) = \lambda_n^{(0)}(r_s)q^2$, all in the limit of small q . Of the three functions $\lambda_s^{(0)}$, $\lambda_a^{(0)}$, and $\lambda_n^{(0)}$ thereby introduced, the combination $\lambda_s^{(0)}(r_s) + \lambda_n^{(0)}(r_s)$ is obtained from the compressibility sum rule, and using the parametrization¹⁵ of the correlation energy from the Green's-function Monte Carlo simulations we have¹⁶

$$\lambda_s^{(0)}(r_s) + \lambda_n^{(0)}(r_s) = 1 + \frac{\pi}{3} \alpha r_s^2 \frac{\partial}{\partial r_s} \epsilon_c - \frac{\pi}{6} \alpha r_s^3 \frac{\partial^2}{\partial r_s^2} \epsilon_c, \quad (38)$$

where $\alpha = (4/9\pi)^{1/3}$ and ϵ_c is the correlation energy expressed in units of Rydbergs. Here $\lambda_a^{(0)}(r_s) + \lambda_n^{(0)}(r_s)$ is given in terms of the spin susceptibility or equivalently by

$$\lambda_a^{(0)}(r_s) + \lambda_n^{(0)}(r_s) = 1 + 3 \left[\frac{2\pi}{3} \right]^{2/3} r_s \frac{\partial^2}{\partial \xi^2} \epsilon_c, \quad (39)$$

where ξ is the spin polarization. On the other hand, in the limit of large w , we know that $G_s(q, iw) = \lambda_s^{(\infty)}(r_s)q^2$, $G_a(q, iw) = -\frac{1}{3}[1 - 2g(0)]$, and $G_n(q, iw) = \lambda_n^{(\infty)}(r_s)q^2$, again, all in the limit of small q . Further $\lambda_s^{(\infty)}(r_s)$ follows

from the third-moment sum rule¹⁶ and is given by

$$\lambda_s^{(\infty)}(r_s) = \frac{3}{5} - \frac{2\pi\alpha}{4} \left[r_s^2 \frac{\partial}{\partial r_s} \epsilon_c = 2r_s \epsilon_c \right]. \quad (40)$$

We can derive a result for $\lambda_n^{(\infty)}(r_s)$ by considering the expression for the modified Lindhard function,

$$\begin{aligned} \bar{\Pi}_0(q, iw) &= \frac{4(k_f a_0)}{a_0^3 (e^2/2a_0)q} \\ &\times \int \frac{d^3k}{(2\pi)^3} n_k \frac{1}{k} \text{Re} \ln \left[\frac{iw - q^2 + 2kq}{iw - q^2 - 2kq} \right]. \end{aligned} \quad (41)$$

For small q and large w , this becomes

$$\begin{aligned} \bar{\Pi}_0(q, iw) &= \Pi_0(q, iw) + \frac{32(k_f a_0)}{a_0^3 (e^2/2a_0)} \frac{q^4}{w^4} \\ &\times \int \frac{d^3k}{(2\pi)^3} (n_k - n_k^0) k^2. \end{aligned} \quad (42)$$

The correction term in this expression is proportional to the difference in the kinetic energy between the interacting and noninteracting systems and this can be related to the correlation energy by the virial theorem. This implies that

$$\lambda_n^{(\infty)} = 3\pi\alpha r_s \frac{d}{dr_s} [r_s \epsilon_c(r_s)]. \quad (43)$$

We determine $\lambda_m^{(0)}(r_s)$ from our numerical calculation by noting that $\lambda_n^{(0)}(r_s) / [\lambda_a^{(0)}(r_s) + \lambda_n^{(0)}(r_s)]$ can be approximately parametrized as

$$\frac{\lambda_n^{(0)}(r_s)}{\lambda_a^{(0)}(r_s) + \lambda_n^{(0)}(r_s)} = \frac{-0.11r_s}{1 + 0.33r_s}. \quad (44)$$

For $r_s < 20$, this parametrization provides a reasonably accurate description of the numerical results of Eqs. (36) and (37). For larger r_s , where Eqs. (36) and (37) are not expected to be very accurate, Eq. (44) underestimates the numerical results. Thus Eq. (44) should be considered as a conservative estimate for $\lambda_n^{(0)}$ for the low-density case. In the limit of large frequency we can show that all three local-field factors possess an extremum for q at or near $w^{1/2}$. For the cases of G_s and G_a , this result follows from the analysis of Niklasson¹⁴ and of Zhu and Overhauser.¹⁷ In particular, their expression for the large- (q, w) limit of the local-field factors, when analytically continued to imaginary frequency reads

$$\begin{aligned} G_{s,a}(q, iw) &= \frac{1}{2N} \sum_{q'} \sum_{\sigma, \sigma'} \left[\alpha(q, w) \frac{(\mathbf{q} \cdot \mathbf{q}')^2 v_{q'}}{q^4 v_q} - \eta_{s,a}(\sigma, \sigma') \right] \\ &\times [S_{\sigma\sigma'}(q') - \delta_{\sigma\sigma'}], \end{aligned} \quad (45)$$

where $\eta_s(\sigma, \sigma') = 1$, $\eta_a(\sigma, \sigma') = \text{sgn}(\sigma \cdot \sigma')$, and $S_{\sigma\sigma'}(q')$ is the static structure factor. The quantity $\alpha(q, w)$ is given by

$$\alpha(q, w) = \frac{1}{2} \frac{(iw + q^2)^2}{(iw - q^2)^2} + \frac{1}{2} \frac{(iw - q^2)^2}{(iw + q^2)^2}. \quad (46)$$

If we differentiate Eq. (45) with respect to q or with

respect to w , we find that maxima occur at $q^2=w$. For the spin-symmetric and spin-antisymmetric local-field factors these maxima are given (for a given density) by

$$\lim_{w \rightarrow \infty} G_s(q^2=w, iw) = \frac{4}{3}[1-g(0)] \quad (47)$$

and

$$\lim_{w \rightarrow \infty} G_a(q^2=w, iw) = \frac{1}{3}[1+2g(0)]. \quad (48)$$

We can show from Eq. (41) that $G_n(q, iw)$ has a minimum at $q^2=(\sqrt{2\sqrt{3}-3})w=0.68w$ with the peak height given by

$$G_n(q=q_{\min}, iw) = 1.180w\pi\alpha r_s \frac{d}{dr_s}[r_s \epsilon_c(r_s)] \quad (49)$$

in the large- w limit. Finally we have the sum rules valid for large q but arbitrary w , namely,

$$\lim_{q \rightarrow \infty} G_s(q, iw) = \frac{2}{3}[1-g(0)], \quad (50)$$

$$\lim_{q \rightarrow \infty} G_a(q, iw) = \frac{4g(0)-1}{3}, \quad (51)$$

and

$$\lim_{q \rightarrow \infty} G_n(q, iw)/q^2 = -\pi\alpha r_s \frac{d}{dr_s}[r_s \epsilon_c(r_s)] = -\frac{1}{3}\lambda_n^{(\infty)}. \quad (52)$$

Equations (35)–(37), though approximate, give a relatively clear guide to the expected form that the local-field factors should take. We now examine the particular qualitative features that should be included in the parametrization. Most importantly there is a peak at $q=1$ for all three of the static local-field factors (see Fig. 3) and at large frequencies, this peak moves out to larger q (see Figs. 4 and 5). In fact, for G_s and G_a at very large w , the peak is actually at $q^2=w$, and we find that for arbitrary

frequency, it is roughly located at $q^2=1+w$. Similarly, for G_n , the peak is roughly located at $q^2=1+0.68w$. The peak in the function $G_n(q, iw)$ diverges toward negative infinity for very large w .

In deciding how to parametrize the local-field factors it is important to use physical information that we expect to remain valid throughout the entire density range, and in most instances this is achieved through use of these sum rules. There is, however, one piece of information that is *not* related to a sum rule, namely, the peak height of the static local-field factors at $q=1$. This region is enhanced by nonanalytic terms which cause the derivative of the local-field factors with respect to momentum to be very large near $q=1$. If we neglect this nonanalytic structure, we find that our *numerical* results are well approximated by taking $G_s(q=1, w=0)=0.9\lambda_s^{(0)}(r_s)$ and $G_a(q=1, w=0)=\lambda_a^{(0)}(r_s)$. Although this somewhat underestimates the peak height near $q=1$, it does allow for a reasonably accurate description for small to intermediate momenta. However, at large r_s , our numerical results are not expected to be very accurate. According to our calculation, for $r_s > 31$ there is a charge-density-wave (CDW) instability. In other calculations,^{18–20} the CDW instability either occurs at much larger r_s or not at all. Therefore, in the case of very low densities the condition $G_s(q=1, w=0)=0.9\lambda_s^{(0)}(r_s)$ should be modified so that the CDW instability occurs at larger r_s . Otherwise in the metallic density range, the condition $G_s(q=1, w=0)=0.9\lambda_s^{(0)}(r_s)$ is expected to be accurate.

Given these considerations, we parametrize the spin-symmetric local-field factors as follows:

$$G_s(q, iw) = \frac{a_s(w)q^2 + b_s(w)\frac{2}{3}[1-g(0)]q^8}{1 + c_s(w)q^2 + b_s(w)q^8}, \quad (53)$$

where, guided by the sum rules, we take

$$b_s(w) = \frac{a_s(w)}{3a_s(w)(1+w)^4 - \frac{8}{3}[1-g(0)](1+w)^3 - 2c_s(w)[1-g(0)](1+w)^4}, \quad (54)$$

$$c_s(w) = \frac{3\lambda_s^{(\infty)}}{4[1-g(0)]} - \frac{\frac{4}{3} - 1/\alpha + \frac{3\lambda_s^{(\infty)}}{4[1-g(0)]}}{1 + \gamma_s w}, \quad (55)$$

and

$$a_s(w) = \lambda_s^{(\infty)} + \frac{\lambda_s^{(0)} - \lambda_s^{(\infty)}}{1 + \gamma_s^2 w^2}. \quad (56)$$

The expression for $b_s(w)$ follows from the condition that the peak height be found at $q^2=1+w$. The expression for $c_s(w)$ results from requiring that the peak height equal $\alpha\lambda_s^{(0)}$ for $w=0$ and $\frac{4}{3}[1-g(0)]$ in the limit of large frequency. The constant γ_s is determined to be $\{9/16[1-g(0)]\}\lambda_s^{(\infty)} + \frac{1}{4} + \frac{3}{4}(1-1/\alpha)$ by requiring the derivative with respect to frequency of $G_s(q, iw)$ vanish when $q^2=w$ for large w . In the following, we will take $\alpha=0.9$, which corresponds to $G_s(q=1, w=0)=0.9\lambda_s^{(0)}(r_s)$. Since the peak height is typically greater than unity in this case, this approximation will result in a CDW instability; we find that this occurs at $r_s=36$. At very low densities it may actually be preferable to use a smaller value of α so that the CDW will occur at lower densities.

We use a very similar procedure to parametrize the spin-antisymmetric local field factors, namely,

$$G_a(q, iw) = -\frac{1}{3}[1-2g(0)] \frac{\gamma_a^2 w^2}{1 + \gamma_a^2 w^2} + \frac{a_a(w)q^2 + b_a(w)\beta(w)q^8}{1 + c_a(w)q^2 + b_a(w)q^8}, \quad (57)$$

where (again guided by the sum rules)

$$b_a(w) = \frac{a_a(w)}{3a_a(w)(1+w)^4 - 4\beta(w)(1+w)^3 - 3c_s(w)\beta(w)(1+w)^4}, \quad (58)$$

$$c_a(w) = \frac{\frac{3}{2}\lambda_a^{(\infty)} - \frac{\frac{1}{3} + \frac{3}{2}\lambda_a^{(\infty)}}{1 + \gamma_a^2 w}}{1 + \gamma_a^2 w}, \quad (59)$$

$$a_a(w) = \lambda_a^{(\infty)} + \frac{\lambda_a^{(0)} - \lambda_a^{(\infty)}}{1 + \gamma_a^2 w^2}, \quad (60)$$

and

$$\beta(w) = \frac{1}{3}[4g(0) - 1] + \frac{1}{3}[1 - 2g(0)] \frac{\gamma_a^2 w^2}{1 + \gamma_a^2 w^2}. \quad (61)$$

The constant γ_a is given by $\frac{2}{3}\lambda_a^{(\infty)} + \frac{1}{4}$.

The local-field factor related to the change in occupation numbers in the Lindhard function is parametrized as

$$G_n(q, iw) = \frac{a_n(w)q^2 + b_n(w)(-\lambda_n^{(\infty)}/3)q^6}{1 + c_n(w)q^2 + b_n(w)q^4}, \quad (62)$$

where

$$b_n(w) = \frac{-3}{2\lambda_n^{(\infty)}(1 + \gamma_n w)^2} (a_n(w) + \lambda_n^{(\infty)} + \frac{2}{3}\lambda_n^{(\infty)}c_n(w)(1 + \gamma_n w) + \{[a_n(w) + \lambda_n^{(\infty)} + \frac{2}{3}\lambda_n^{(\infty)}c_n(w)(1 + \gamma_n w)]^2 + \frac{4}{3}a_n(w)\lambda_n^{(\infty)}\}^{1/2}), \quad (63)$$

$$c_n(w) = \frac{3\gamma_n(w)}{1.18(1 + \gamma_n w)} - \left\{ \frac{\lambda_n^{(0)} + \frac{1}{3}\lambda_n^{(\infty)}}{\lambda_n^{(0)} + \frac{2}{3}\lambda_n^{(\infty)}} + \frac{3\gamma_n(w)}{1.18(1 + \gamma_n w)} \right\} \frac{1}{1 + \gamma_n^2 w^2}, \quad (64)$$

and

$$a_n(w) = \lambda_n^{(\infty)} + \frac{\lambda_n^{(0)} - \lambda_n^{(\infty)}}{1 + \gamma_n^2 w^2}. \quad (65)$$

The constant γ_n is 0.68. The procedure we use to determine the parametrization for G_n is very similar to the procedures used to parametrize the other local-field factors.

In Figs. 3–5, the results for the local-field factors are shown. The discrepancies between our parametrization of the local-field factors and the numerical calculation arise primarily for two reasons. First, as expected, the results of the *numerical* calculation do not exactly satisfy the sum rules; this leads to a fairly large error in the large- q results from the numerical calculation. Second, the parametrization neglects the sharp peak in the static local-field factors at $q = 1$. Because they satisfy the sum rules, the parametrized local-field factors *can* be expected to be more accurate than the numerically calculated local-field factors at metallic and lower densities. As shown in Fig. 6, the effective potentials resulting from the use of both the parametrized and the numerical local-field factors are actually not very different.

IV. EFFECTIVE ELECTRON-ELECTRON INTERACTIONS

As noted above, in many problems in condensed-matter physics involving electronic structure, it is useful

to describe the many-body effects of screening, exchange, and correlation in terms of an effective two-body electron-electron interaction. A physically motivated expression for this effective interaction in the interacting electron-gas problem has already been given by Kukkonen and Overhauser.¹ Their expression is derived by considering the rearrangement of electrons in the vicinity of a test charge; the rearranged electrons constitute a charge cloud which interacts with other particles through a direct Coulomb term, but also through an exchange term which is proportional to the local-field factor. The KO result can be written

$$V_{\sigma\sigma'}^{\text{eff}}(\vec{q}) = \Lambda^2(\vec{q}) \frac{v_q}{\epsilon(\vec{q})} + \frac{[v_q G_s(\vec{q})]^2 \bar{\Pi}_0(\vec{q})}{1 + v_q (G_s(\vec{q}) \bar{\Pi}_0(\vec{q}))} + \sigma \cdot \sigma' \frac{[v_q G_a(\vec{q})]^2(\vec{q}) \bar{\Pi}_0(\vec{q})}{1 + v_q G_a(\vec{q}) \bar{\Pi}_0(\vec{q})}, \quad (66)$$

where v_q is the bare Coulomb interaction, $\Lambda(\vec{q})$ is the vertex function and is given by

$$\Lambda(\vec{q}) = \frac{1}{1 + v_q G_s(\vec{q}) \bar{\Pi}_0(\vec{q})}, \quad (67)$$

σ are the Pauli matrices, and $\epsilon(\vec{q})$ is the dielectric function, given by

$$\epsilon(\vec{q}) = 1 - v_q \bar{\Pi}_0(\vec{q}) \Lambda(\vec{q}). \quad (68)$$

Vignale and Singwi have also derived similar expres-

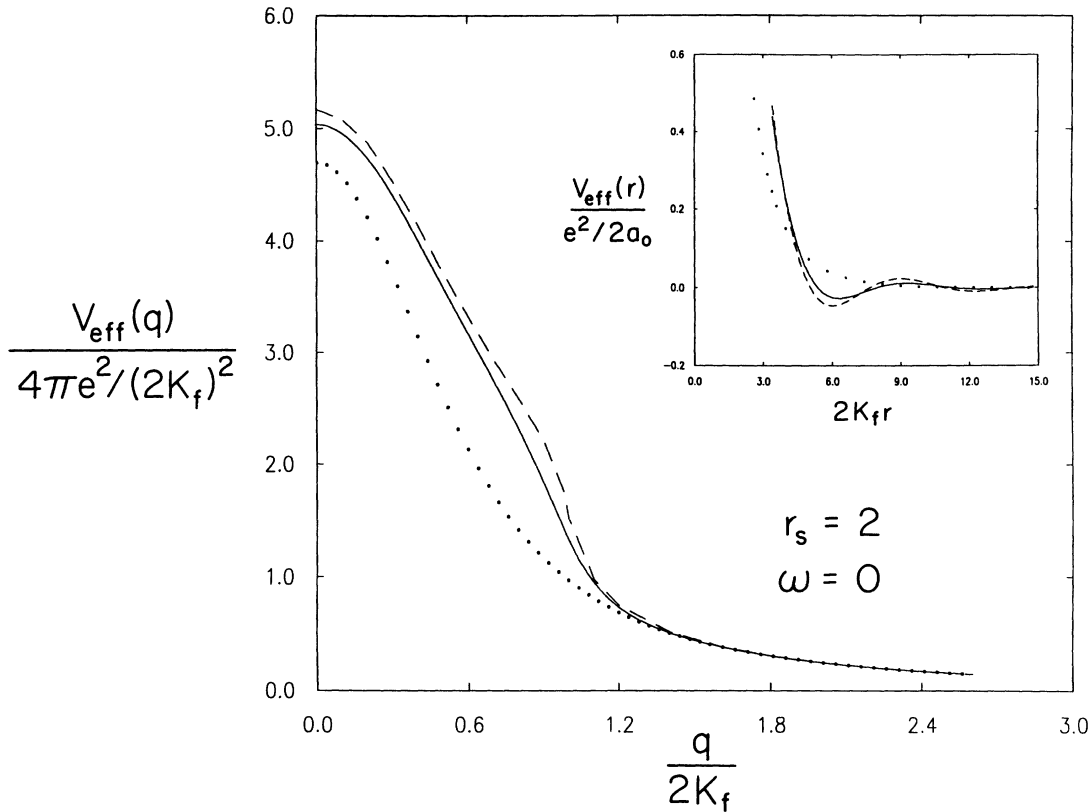


FIG. 6. Effective electron-electron interaction from Eqs. (66) with $r_s=2$ and $w=0$. The inset shows the corresponding real-space behavior of the effective interaction. The solid lines are calculated using the local-field factors defined in Eqs. (53)–(65), the dashed lines are calculated using the local-field factors defined in Eqs. (35)–(37), and the dotted lines are calculated using the local-field factors of Takada (Ref. 20).

sions based on a diagrammatic study of the irreducible particle-particle interaction.¹⁰ In their theory, ladder diagrams are summed in the local approximation, and their results give precisely the same V_{ss}^{eff} as the KO expression, but augmented by an additional term representing transverse spin fluctuations, namely,

$$V_{s-s}^T(\tilde{p}_1, \tilde{p}_2, \tilde{q}) = 2 \frac{(vG_a)^2 \bar{\Pi}_0}{1 + vG_a \bar{\Pi}_0}. \quad (69)$$

This term is incorporated into the irreducible particle-particle interaction J in the following manner:

$$J_{ss}(\tilde{p}_1, \tilde{p}_2, \tilde{q}) = V_{ss}^{\text{eff}}(\tilde{q}) - V_{s-s}^{\text{eff}}(\tilde{p}_1 - \tilde{p}_2 - \tilde{q}) \quad (70)$$

and

$$J_{s-s}(\tilde{p}_1, \tilde{p}_2, \tilde{q}) = V_{s-s}^{\text{eff}}(\tilde{q}) - V_{s-s}^T(\tilde{p}_1 - \tilde{p}_2 - \tilde{q}). \quad (71)$$

The term representing the transverse spin fluctuations is not present in the KO expression because the KO formalism is a strictly local formalism and therefore cannot lead to terms which depend on the transverse momentum transfer. However, for the case of the gap equation for superconductivity, Vignale and Singwi²¹ have shown that their expression for the effective interaction is approximately equivalent to the KO expression. Since one of the more interesting applications^{2,20} of the effective interac-

tion is indeed in the area of superconductivity, we will use the form of the effective interaction that is appropriate for the kernel in the gap equation, namely, Eq. (66). Note that the spin fluctuations mediate a repulsive interaction for singlet pairing, but an *attractive* interaction for triplet pairing. Note also that the local-field factors play a crucial role.

In Fig. 6, we compare the static effective interaction obtained from Eq. (66) using the local-field factors derived here with the static effective interaction obtained using the Hubbard-like parametrization of Takada.²⁰ It is because the fully interacting particle numbers n_k are used in our calculation through the local-field factor G_n that the effective interaction is larger in our case for the $q=0$ limit. If we ignore G_n , we find that the effective interaction is then equal to Takada's result at $q=0$, but at higher q , our effective interaction is considerably larger than that predicted by Takada's approximation. The discrepancy for immediate wave vectors results directly from the peaked structure of the local-field factors apparent in Fig. 3. The effective interaction in real space is also shown in Fig. 6. The Friedel oscillations are much larger in our approximation than in Hubbard-like approximations because of the peak in the local-field factors at $q=1$. In Fig. 7, we plot the effective interaction as a function of frequency. From the difference in frequency dependence of the effective interaction shown in this

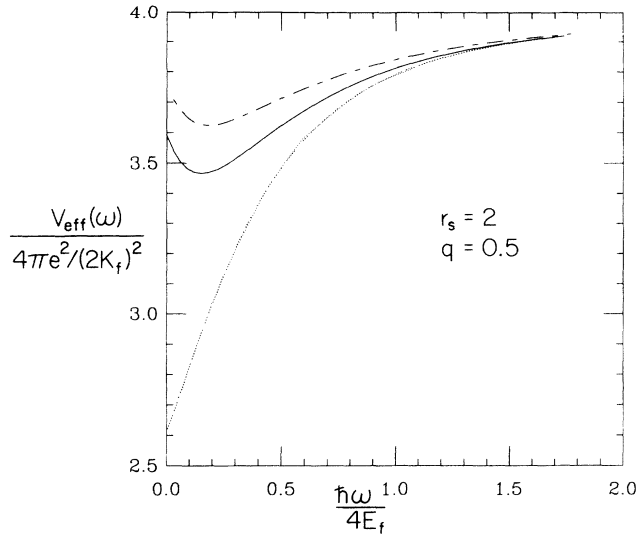


FIG. 7. Effective electron-electron interaction from Eq. (66) for $r_s=2$ and $q=0.5$. The solid line is calculated using the local-field factors defined in Eqs. (53)–(65), the dashed line is calculating using the local-field factors defined in Eqs. (35)–(37), and the dotted line is calculated using the local-field factors of Takada (Ref. 20).

figure, it is clear that it is necessary to use frequency-dependent local-field factors in order to accurately predict the effective interaction.

V. CONCLUSIONS

We have calculated the local-field factors using an integral equation to sum an infinite number of diagrams for the response functions. The results for the local-field factors have been related to low-order polarization diagrams. We reduced the first-order diagrams to one-dimensional integrals and the higher-order diagrams were related to three-dimensional integrals involving the three-point function. It was necessary to associate some self-energy terms with a new local-field factor which we used to modify the Lindhard function to include the effects of correlations on the particle occupation number. We then suggested a parametrization scheme to simplify the calculation of the local-field factors and to make sure that they satisfy the known sum rules. We have also found new sum rules showing that for large $i\omega$, the local-field factors have a peak at or near $q^2=w$ and the peak height is related to the radial distribution function at zero separation.

We used the local-field factors to calculate the effective electron-electron interaction and as a consequence we observe several significant differences between our result and results obtained using Hubbard-like local-field fac-

tors. The effective interaction obtained using the local-field factors which we derived is considerably larger for $q < 1$ and $w < 1$ than the effective interaction obtained using Hubbard-like local-field factors because of the proper inclusion of particle number renormalization in our description and because of the peaked structure of our local-field factors near $q = 1$. Our conclusion is that it is necessary to use local-field factors which have a peaked structure, are frequency dependent, and include the effects of correlation on the electron occupation numbers to correctly predict the effective electron-electron interaction.

An interesting problem where the effective electron-electron interaction is clearly required is the question of intrinsic superconductivity in the electron gas.^{2,20} This problem has been addressed by Takada²⁰ using simple Hubbard-like forms for the local-field factors. The results of the present paper provide a more accurate effective electron-electron interaction which can be used in the Eliashberg equation to predict the temperature where a superconducting transition could occur. This matter will be dealt with at more length in a separate publication.²

ACKNOWLEDGMENTS

This work was supported in part by the National Science Foundation through Grant No. DMR-9017281. C.F.R. wishes to thank the Department of Energy for financial support.

APPENDIX

Derivation of the three-point function

The three-point function is defined in Eq. (26). We can carry out a simple frequency integral to obtain¹³

$$\Lambda_0^{(3)}(\vec{q}, \vec{p}) = -I(\vec{q}, \vec{q} + \vec{p}) - I(-\vec{q}, \vec{p}) + I(-\vec{q} - \vec{p}, -\vec{p}), \quad (\text{A1})$$

where

$$I(\vec{q}, \vec{p}) = \frac{2}{a_0(e^2/2a_0)(k_f a_0)} \times \int \frac{d^3k}{(2\pi)^3} \Theta(\frac{1}{2} - k) \frac{1}{q^2 + 2\mathbf{k} \cdot \mathbf{q} - i\omega_q} \times \frac{1}{p^2 + 2\mathbf{k} \cdot \mathbf{p} - i\omega_p}. \quad (\text{A2})$$

As written, the angular integrals in this expression are difficult to evaluate. To simplify them we use the so-called ‘‘Feynman trick’’ to combine the two terms in I into a single term, according to

$$I(\vec{q}, \vec{p}) = \frac{\pm 2}{a_0(e^2/2a_0)(k_f a_0)} \int \frac{d^3k}{(2\pi)^3} \Theta(\frac{1}{2} - k) \int_0^1 dx [\pm(q^2 - i\omega_q)(1-x) + (p^2 - i\omega_p)x + 2\mathbf{k} \cdot \mathbf{q}(1-x) \pm \mathbf{k} \cdot \mathbf{p} \cos(\theta)]^{-2}. \quad (\text{A3})$$

In Eq. (A3), the plus (minus) sign is chosen if $\omega_q \cdot \omega_p$ positive (negative). This ensures that there is no singularity in the

integrand and that the order of integration can be changed. After integrating over angles we have

$$I(\bar{q}, \bar{p}) = \frac{\pm 1}{2\pi^2 a_0 (e^2/2a_0)(k_f a_0)} \int_0^{1/2} k^2 dk \int_0^1 dx \{ [\pm(q^2 - iw_q)(1-x) + (p^2 - iw_p)x]^2 - 4k^2 |q(1-x) \pm px|^2 \}^{-1}. \quad (\text{A4})$$

We write the denominator of Eq. (A4) as $(a_0 - a_1 k^2) + 2(b_0 - b_1 k^2)x + (c_0 - c_1 k^2)x^2$. The x integral can then be easily be performed giving

$$I(\bar{q}, \bar{p}) = \frac{\pm 1}{4\pi^2 a_0 (e^2/2a_0)(k_f a_0)} \int_0^{1/2} k dk \frac{1}{[\alpha + \beta k^2]^{1/2}} \left\{ \ln \left[\frac{c_0 + b_0 - (c_1 + b_1)k^2 - k[\alpha + \beta k^2]^{1/2}}{b_0 - b_1 k^2 - k[\alpha + \beta k^2]^{1/2}} \right] - \ln \left[\frac{c_0 + b_0 - (c_1 + b_1)k^2 + k[\alpha + \beta k^2]^{1/2}}{b_0 - b_1 k^2 + k[\alpha + \beta k^2]^{1/2}} \right] \right\}, \quad (\text{A5})$$

where $\alpha = (a_0 c_1 + c_0 a_1 - 2b_0 b_1)$ and $\beta = b_1^2 - a_1 c_1$. By writing

$$\frac{k}{[\alpha + \beta k^2]^{1/2}} = \frac{1}{\beta} \frac{\partial}{\partial k} [\alpha + \beta k^2]^{1/2}, \quad (\text{A6})$$

we can integrate by parts to obtain

$$I(\bar{q}, \bar{p}) = \frac{\pm 1}{4\pi^2 \beta a_0 (e^2/2a_0)(k_f a_0)} \times \left\{ [\alpha + \beta/4]^{1/2} \left[\ln \left[\frac{c_0 + b_0 - (c_1 + b_1)/4 - 1/2[\alpha + \beta/4]^{1/2}}{b_0 - b_1/4 - 1/2[\alpha + \beta/4]^{1/2}} \right] - \ln \left[\frac{c_0 + b_0 - (c_1 + b_1)/4 + 1/2[\alpha + \beta/4]^{1/2}}{b_0 - b_1/4 + 1/2[\alpha + \beta/4]^{1/2}} \right] \right] + \frac{\tau C + \sigma f}{2h(Cf)^{1/2}} \{ \ln[1 - \frac{1}{2}C/(Cf)^{1/2}] - \ln[1 + \frac{1}{2}C/(Cf)^{1/2}] \} - \frac{\tau C + \sigma g}{2h(Cg)^{1/2}} \{ \ln[1 - \frac{1}{2}C/(Cg)^{1/2}] - \ln[1 + \frac{1}{2}C/(Cg)^{1/2}] \} \right\}, \quad (\text{A7})$$

where $h = (B^2 + 4AC)^{1/2}$, $f = B/2 + h/2$, $g = B/2 - h/2$, $A = (c_0 + b_0)^2$, $B = -2(c_0 + b_0)(c_1 + b_1) - \alpha$, $C = \beta - (c_1 + b_1)^2$, $\tau = 2\alpha(c_0 + b_0)$, and finally $\sigma = 2\alpha(c_1 + b_1) + 4\beta(c_0 + b_0)$.

- ¹C. A. Kukkonen and A. W. Overhauser, Phys. Rev. B **20**, 550 (1979).
²C. F. Richardson and N. W. Ashcroft (unpublished).
³G. Baym and L. P. Kadanoff, Phys. Rev. **124**, 287 (1961).
⁴S. S. Jha, K. K. Gupta, and J. W. F. Woo, Phys. Rev. B **4**, 1005 (1971).
⁵A. K. Rajagopal, Phys. Rev. A **6**, 1239 (1972).
⁶F. Brosens, L. F. Lemmens, and J. T. Devreese, Phys. Status Solidi B **74**, 45 (1976); **81**, 551 (1977); **82**, 117 (1977); F. Brosens, J. T. Devreese, and L. F. Lemmens, *ibid.* **80**, 99 (1977).
⁷J. T. Devreese, F. Brosens, and L. F. Lemmens, Phys. Rev. B **21**, 1349 (1980).
⁸G. Vignale, Phys. Rev. B **38**, 6445 (1988).
⁹H. B. Singh and K. N. Pathak, Phys. Rev. B **10**, 2764 (1974).

- ¹⁰G. Vignale and K. S. Singwi, Phys. Rev. B **32**, 2156 (1985).
¹¹C. A. Kukkonen and J. W. Wilkins, Phys. Rev. B **19**, 6075 (1979).
¹²E. Engel and S. H. Vosko, Phys. Rev. B **42**, 4940 (1990).
¹³R. Cenni and P. Saracco, Nucl. Phys. A **487**, 279 (1988).
¹⁴G. Niklasson, Phys. Rev. B **10**, 3052 (1974).
¹⁵S. H. Vosko, L. Wilk, and M. Nusair, Can. J. Phys. **58**, 1200 (1980).
¹⁶N. Iwamoto, Phys. Rev. B **30**, 3289 (1984).
¹⁷X. Zhu and A. W. Overhauser, Phys. Rev. B **30**, 3158 (1984).
¹⁸H. K. Schweng and H. M. Bohm, Phys. Rev. B **48**, 2037 (1993).
¹⁹N. Iwamoto and D. Pines, Phys. Rev. B **29**, 3924 (1984).
²⁰Y. Takada, Phys. Rev. B **47**, 5202 (1993).
²¹G. Vignale and K. S. Singwi, Phys. Rev. B **31**, 2729 (1985).